DOI: 10.1007/s12541-011-0061-4

A Study on Optimal Design and Fatigue Life of the Common Rail Pipe

Jun-Ho Bae[1], Moon-Saeng Kim[2], Myung-Jun Song[2], Sung-Yuen Jung[2] and Chul Kim[2,#]

1 School of Mechanical Engineering, Pusan National University, San30, Jangjeon-dong, Geumjeong-gu, Busan, South Korea, 609-735
2 Research Institute of Mechanical Technology, Pusan National University, San30, Jangjeon-dong, Geumjeong-gu, Busan, South Korea, 609-735
Corresponding Author / E-mail: chulki@pusan.ac.kr, TEL: +82-51-510-2489, FAX: +82-51-512-9835

KEYWORDS: Common Rail Pipe, Folding Defect, Heading process, Fatigue life, FE-simulation

To support the latest automobile technology, the next generation of diesel engines is expected to require higher injection pressures than the third generation which can operate at high injection pressures up to 1,800bar. A component in the common rail system, the common rail pipe must have higher strength because it is directly influenced by the high-pressure fuel. Preform design is very important for preventing the head of the common rail pipe from folding in the heading process. In this study, the angle, curvature and outer diameter of the die and the length of the trapped part are selected as main parameters in the design of the optimal preform shape that minimizes the radius of folding. The optimal design is carried out by finite element analysis and the Taguchi method using the main parameters and then fatigue-life analysis is preformed for predicting fatigue life according to the amount of folding. Also, a closed form equation to predict fatigue life was suggested by Goodman theory and life-prediction method for pressure vessels pursuant to ASME Code. In order to verify the reliability of common rail pipe, fatigue-structural coupled field analysis is performed. The results of the finite element analysis were in good agreement with those of the experiments at the actual site and theoretical analysis.

Manuscript received: January 29, 2010 / Accepted: October 24, 2010

1. Introduction

Fuel induction is controlled by the common rail system for fuel injection pressures of up to 1,600bar. A common rail system is shown in Fig. 1. A diesel engine with the direct injection is more fuel-efficient than a gasoline engine, but it is heavy, and it causes smog, loud noise, and vibrations. Thus, the improvement in the performance of the common rail system has been studied extensively since the 1990s. Fuel injection system greatly affects the performance of a direct injection diesel engine. A common rail injection system was introduced to meet the stringent emission standards, and the low fuel consumption, low noise requirements that have been enforced in recent years. The performance of a common-rail fuel injection system is strongly influenced by the injector characteristics. The design of common rail injector has evolved to improve its injection performance.

Many studies introduced the common rail direct injection (CRDI) system to increase engine power, improve fuel efficiency, and reduce noise, vibration and auto exhausts. In 1997, R. Bosh adapted the high speed direct injection (HSDI) method to diesel engines, and the engines were produced afterwards with further investigation.[1]

In the CRDI system, over 1600bar of high pressure is present in the common rail pipe, when high-pressure fuel is passing through from hydraulic accumulator, called Rail, to the injector.

The joint of the common rail pipe used under high pressure, is produced by the heading process. In relation to the hollow upsetting and heading process, the analysis for the defect in the final shape of the pipe in response to the initial shape, and the impact of the defect on the material flow due to the change in the friction factor of die-work piece interface are studied.[2-4]

During the heading process, the exterior defects that are produced only lead to inferior goods, but interior defects, such as a minute defect of the deformed zone, can cause cracks or fractures in the pipe because these defects are affected by the high fuel pressure. Hence, trial and error is used to minimize the number of folding defects in the common rail pipes.

In this study, the angle, curvature and outer diameter of the die and the length of the trapped part are selected as main parameters in the optimal design of the preform shape that minimizes the radius of folding. The optimal design is determined by finite element analysis and the Taguchi method using the main parameters. The structural analysis of fuel oil supply pipe of common rail system, to applied the optimal design of the preform shape is performed

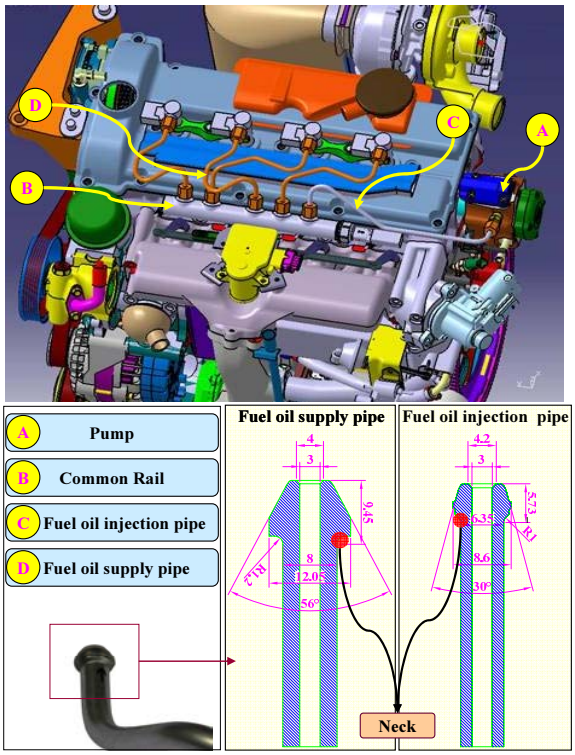

Fig. 1 Common rail system

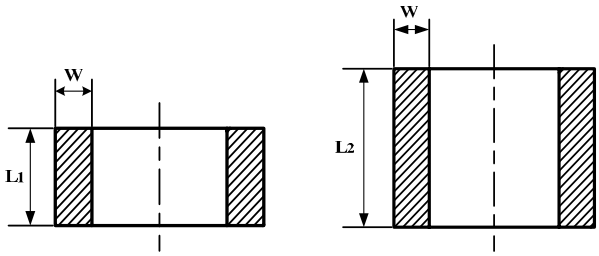

(a) None Used mandrel (b) Used mandrel

Fig. 2 Influence on the mandrel in tube upsetting criteria

according to not only the current heading process(a one-stage process) but also the improved heading process(a two-stage process). A fatigue-life of the fuel oil supply pipe is analyzed according to the size of folding radius occurring in the pipe forming process. Also, theoretical fatigue life is calculated by life-prediction method for pressure vessels pursuant to ASME Code.[5,6] The results of fatigue analysis by FE-simulation were compared with those of theoretical analysis and verified.

2. Die Design and Forming Analysis

Generally, if the diameter to height ratio of a common rail pipe is under 2.25, one-stage upsetting occurs, but if it is in between 2.25 and 4.5, two-stage upsetting occurs, according to the rules of solid and hollow upsetting.

Eq. (1) and (2) are applied to the heading process. The maximum length of the billet that would not cause any defects can be 1.75 to 2 times greater than the thickness of the material.[7] If mandrel is used, the length can be 3.3 times greater than the

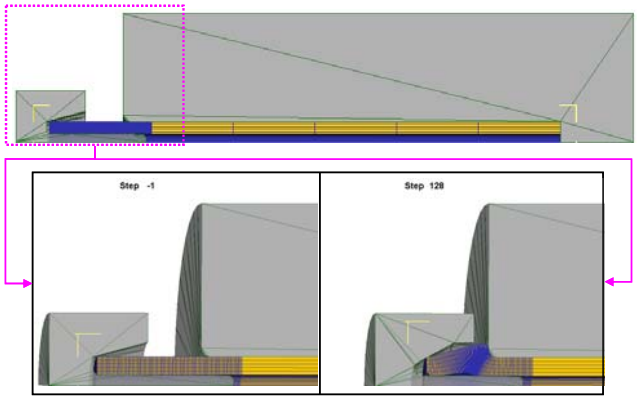

Fig. 3 Modelling for a two-stage heading process

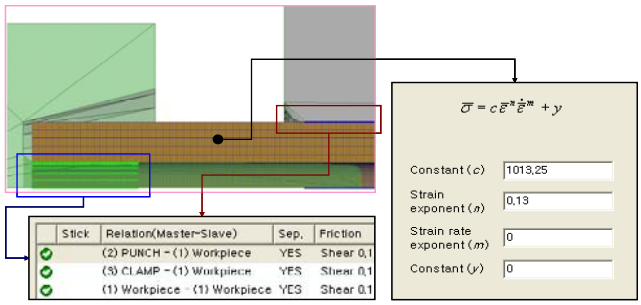

Fig. 4 Boundary condition for the first step, pre-upsetting

thickness of the material. Thus, in the common rail pipe manufacturing process, Eq. (2) has to be used.

$$L_1 = 1.75 \times W, \quad L_1 = 2 \times W \tag{1}$$

$$L_2 = 3.3 \times W \tag{2}$$

From the volume of the final pipe shape, the forming length of the initial shape is calculated to be 14.37mm. However, according to Eq. (2), non-defect-causing length has to be 8.25mm. Therefore, the first-stage heading process has to be followed by the second-stage to minimize defects, and the optimal preform design by the first pre-upsetting process is required.[8-11]

To reduce the FEM computational time, only one quadrant of the cross-section of product is considered as shown in Fig. 3. The shape optimization of the preform dies in a two-stage heading process yielded two shapes for the pre-form punch model.

The preform shape and the final shape of the punch model are applied to the first-stage of the pre-upsetting process and the second-stage of the heading process respectively. In a real process, the clamp is joint-connected to the pipe, but in FEM, in order to simplify the process, a single-body clamp is applied, and the lower part of the clamp is modelled as a support for a material. In the forming analysis of heading process, the transformation hysteresis of the pre-upsetting material is constant, and the same clamp model is applied.

The boundary conditions in the FEM are shown in Fig. 4. The length of the specimen is 100mm, and the grid density of the heading part is higher than the other parts.

The grid density in the folding part affects the final internal shape. Also, punch and clamps are set to be rigid bodies. The punch

Table 1 Mechanical property of ST52

Young's Modulus	2.12 X 105 MPa
Poisson's Ratio	0.285
Mass Density	7.85 X 10-6 kg/mm^3
Tensile Yield Strength	600 MPa
Tensile Ultimate Strength	700 MPa
Plastic coefficient	1013.25 MPa
Strain hardening coefficient	0.13

stroke is taken every 0.05mm in order to observe the micro deformation of the material in the die. The friction value among the punch-billet-clamp is set as a constant, 0.1.

$$\bar{\sigma} = 1013.25\varepsilon^{0.13} \text{ [MPa]} \quad (3)$$

Eq. (3), representing the flow stress curve drawn from the curve fitting, is applied in the forming analysis. The mechanical properties are given in Table 1.

3. Optimal Design for Preform Punch

3.1 Taguchi Method

The optimal design of the preform punch is performed by Taguchi method. The angle (α), curvature (ρ) and outer diameter of the die (D2) and the length of the trapped part (L1) are selected as design variables of preform punch for the optimal design of the preform shape that minimizes the radius of folding as shown in Fig. 5. Notch growth of folding zone at the inner surface of the pipe caused by the heading process is highly associated with the strain in radial direction. So radial strain is selected to the objective function, and the location which is considered is the region with the maximum radial strain in the folding zone.

Because the smaller strain is the better prevention of folding defects, smaller-the-better-characteristic is defined as the loss function, and the ratio of S/N (signal-to-noise) can be calculated by Eq. (4) as follows, where n and y are the number of the data and the measured values respectively.[12,13]

$$S/N = -10\text{Log}\left(\frac{1}{n}\sum_{i=1}^{n} y_i^2\right) \quad (4)$$

The control factors for the design of experiment are level 3. These are based on the data obtained by operator experience, which satisfy the volume consistency and the Eq. (2). The design of experiment is based on the following values, and the measured values are shown in Table 2.

From the results of the orthogonal array, the S/N ratio for the smaller-the better characteristic of strain can be found, and it is shown as a graph in Fig. 6.

The optimal shape of the preform punch for the larger S/N ratio corresponds to L1=6.12 mm, D2=11.0mm, α =46°, and ρ=10mm as shown in Fig. 6. By using these values, the final heading process results are illustrated in Fig. 7. Fig. 7 indicates the maximum deformation points with A, B, and C in each section.

As a result, the strain is 0.809 at the folded area. Compared to the values in Table 2, this value of strain confirms the safety design.

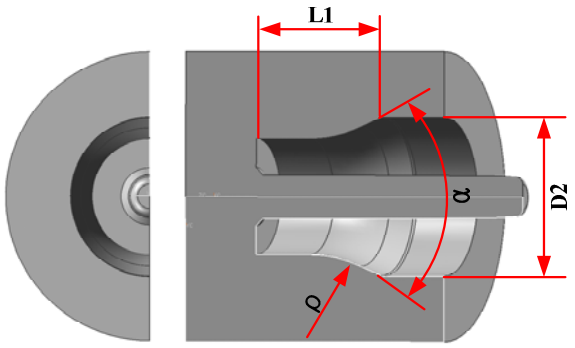

Fig. 5 Design variables of preform punch for design of experiment

Table 2 L9(3^4) orthogonal array for design of experiments

Case	L1(mm)	D2(mm)	α(°)	ρ(mm)	Strain
1	5.62	11.0	42	6	0.844
2	5.62	11.2	46	8	0.822
3	5.62	11.4	50	10	0.840
4	5.87	11.0	46	10	0.816
5	5.87	11.2	50	6	0.867
6	5.87	11.4	42	8	0.841
7	6.12	11.0	50	8	0.844
8	6.12	11.2	42	10	0.825
9	6.12	11.4	46	6	0.834

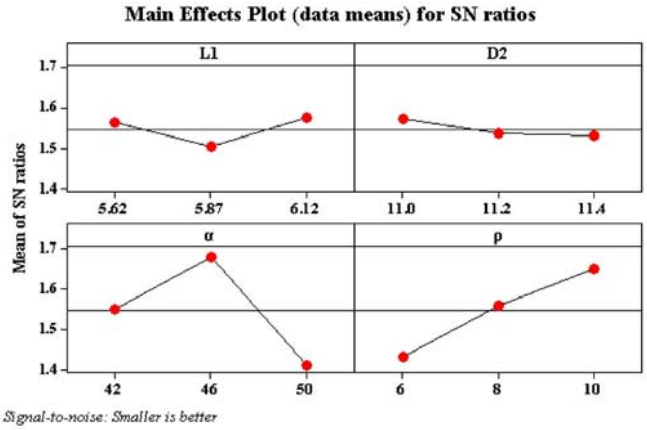

Fig. 6 Effect of design variables on the strain

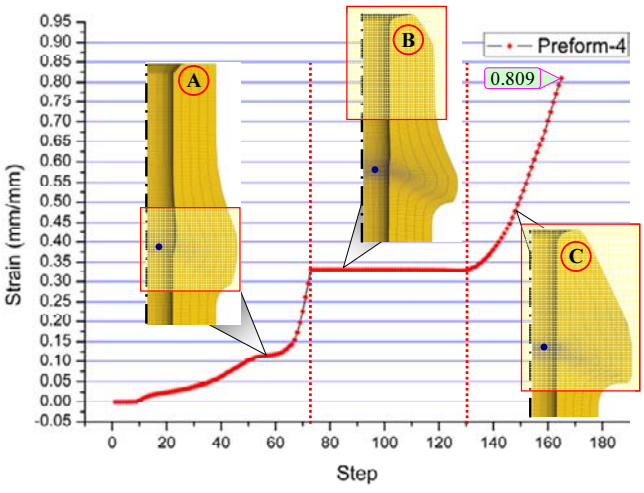

Fig. 7 The results carried out by finite element analysis with the optimal design values

Fig. 8 Preform punch manufactured by the finite element analysis and the design of experiment

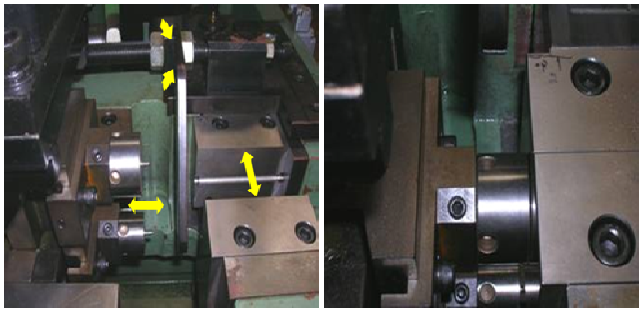

Fig. 9 The equipment of heading process

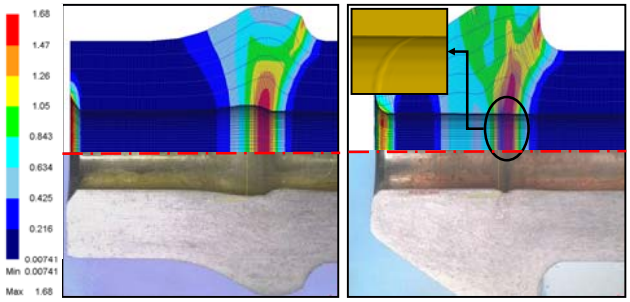

Fig. 10 Comparison of equivalent strain of FEM in with those of experiments

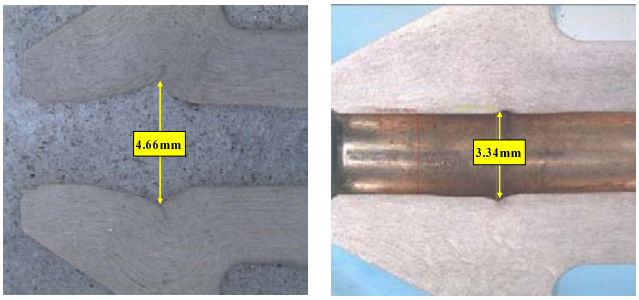

(a) Shape of folding defect (one-stage process) (b) Improved shape of folding defect (two-stage process)

Fig. 11 Cross-Section of the head parts

3.2 Interpretation and Comparison with the Experimental Result

In order to compare the simulated results with the experimental results, experiments with preform punches from the pipe-billet were conducted. Fig. 8 shows the shape of the preform punch manufactured with application of the simulated results and the design of experiments.

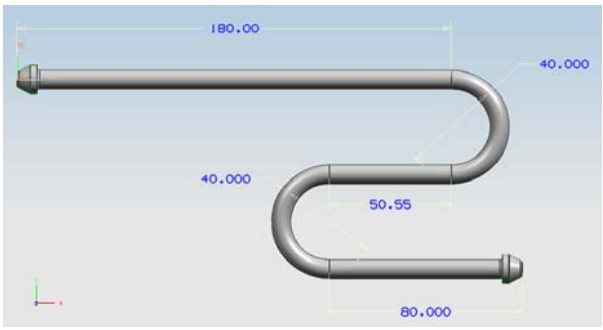

Fig. 12 Shape and dimensions of pipe for stability test

Fig. 9 illustrates the heading process carried out by a multi-stage former where the clamp fixes the pipe-billet, and the stopper controls the forming length during the operation. After the pipe is fixed, the first punch, which is installed on the multi-stage former, forms the preform, and then the second punch forms the final product.

Fig. 10 shows the equivalent strain and the tendency of the folding defect of preform in the pre-upsetting process and heading process. The lower and the upper parts of Fig. 10 show the experiment results and FEM analysis results respectively. Left part of the figure shows the half cross-section of the folding zone and outer geometry formed by preform punch. Right part shows the shape of the final product after completion of the heading process. And the final inner shapes were magnified to show the characteristics of the folding zone in detail. In the pre-upsetting process, the outer diameter of the folding zone is 3.44mm from experiment and 3.14mm from FEM. In the heading process, the outer diameter of folding zone is 3.34mm from experiment and 3.05mm from FEM. The defect tendency in FEM is good agreement with that in the experiment.

Also, the outer diameter of folding zone in the current heading process (a one-stage process) is compared with that of folding zone in the improved heading process (a two-stage process) by experiment. The cross-sections of the head part according to the each heading process are shown in Fig. 11. In a one-stage heading process, the folding defect is occurred and the maximum diameter of folding zone is 4.66mm. In a two-stage heading process, the folding defect is not occurred and the maximum diameter of folding zone is 3.34mm. To prevent the folding defect through the folding process of fuel oil supply pipe, a one-stage heading process is needed to be modified to a two-stage process.

4. Structural Analysis of Common Rail pipe

4.1 Modeling and Boundary Condition

In the stability test of fuel oil supply pipe, each end of the pipe is tightened as bolts, and then the test is performed under the higher inner pressure than the injection pressure from fuel pump. The shape and dimension of the pipe are shown in Fig. 12.

To reduce the computation time, the 1/2 symmetric condition is applied to the FE-simulation model. Also, to minimize numerical error and represent accurate geometry, the elements for folding

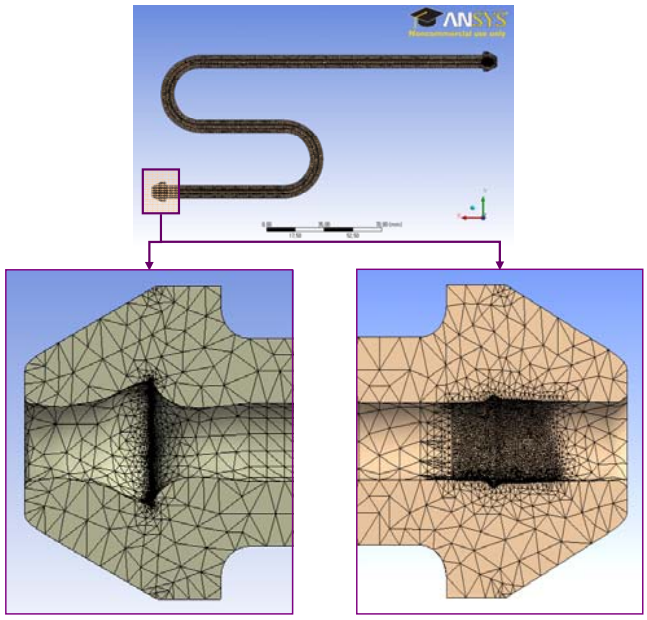

(a) Shape of folding defect (one-stage process) (b) Improved shape of folding defect (two-stage process)

Fig. 13 Meshing for structure analysis

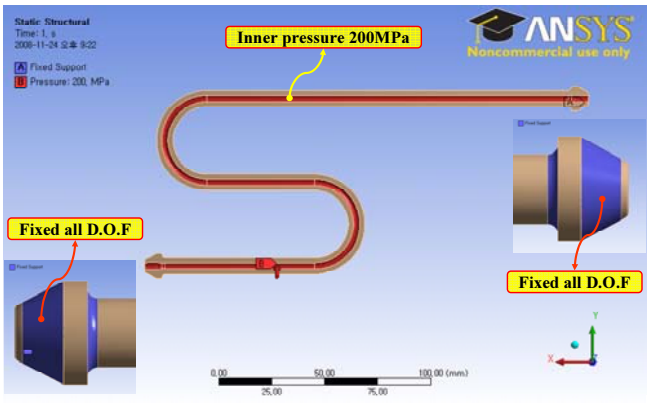

Fig. 14 Boundary conditions for FEM

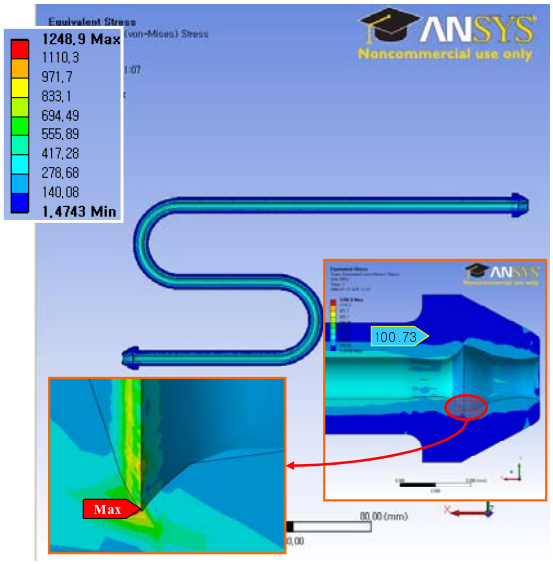

(a) Shape of folding defect

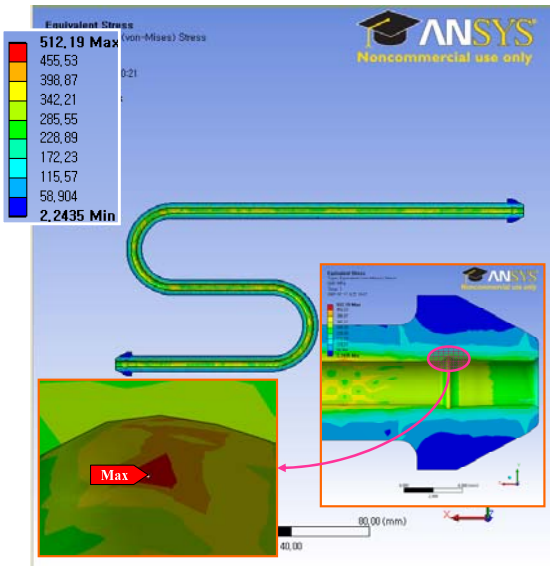

(b) Improved Shape of folding defect

Fig. 15 Stress distribution according heading processes

defect part are densely created than the other parts as shown in Fig. 13. The material of the fuel oil supply pipe is ST_52 and its properties are shown in Table 1.

The both ends of the pipe model are fixed in all D.O.F for the same condition as the bolted joint as shown in Fig. 14. The inner pressure in the pipe is the testing pressure (200MPa), which is higher than the actual working pressure (160 ~ 180MPa).

4.2 Analysis Results and Discussion

The analysis results according to before and after improvement of the heading process are shown in Fig. 15.

In the current heading process (a one-stage process), the stress concentration, the maximum stress is 1,248.9MPa, occurs at the end of folding zone. The value of maximum stress is larger than the yield strength (600MPa) of the material, ST_52. So, the end of folding zone will be the starting point of crack propagation. However, in the improved heading process (a two-stage process), the maximum stress, 512.19MPa, is reduced by more than 50%. These results show that the shape and diameter size of folding part are the important factors under the inner high pressure influencing the failure of the supply pipe in the common rail system.

5. Fatigue Life

5.1 Theoretical Analysis

Theoretical fatigue analysis of the fuel oil supply pipe in the common rail system is based on the fatigue theory of pressure vessel in ASME Code, and the equivalent stress is used with the result of structural analysis. The procedure for fatigue life-prediction by the FEM and the theoretical analysis is shown in Fig. 16.

The mean stress for low cycle fatigue analysis, when the inner pressure is applied at the pipe, is not the same as the value directly calculated from the applied load. So, the mean stress should be modified for fatigue analysis[5] because the original S-N curve is obtained from the test performed under the condition that the modified mean stress is zero.[14]

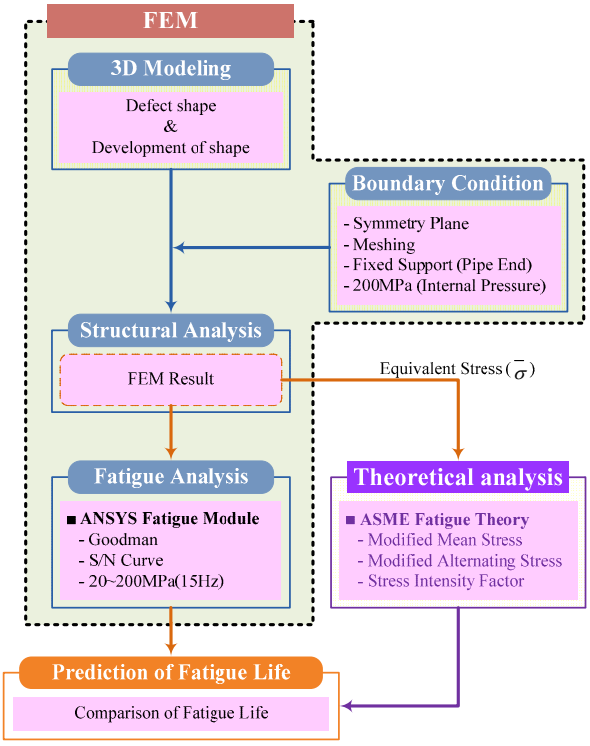

Fig. 16 The procedure of fatigue evaluation for FEM and theoretical analysis

Goodman equation is Eq. (5), where the mean stress (σ_m) is zero, and stress amplitude (S_a) is Eq. (6). Also modified stress amplitude ($S_a^{'}$) is Eq. (7), and the modified mean stress ($S_m^{'}$) is Eq. (9) determined by Eq. (8). Finally, modified alternating stress ($\sigma_a^{'}$) is Eq. (10).[15]

$$\frac{\sigma_a}{S_a}+\frac{\sigma_m}{S_u}=1 \tag{5}$$

$$\sigma_a = S_a = \frac{1}{2}(\sigma_{Max}-\sigma_{Min}) \tag{6}$$

$$S_a^{'} = \frac{1}{2}K\cdot\frac{(\sigma_{\max}-\sigma_{\min})}{2} \tag{7}$$

$$S_m = \frac{(\sigma_{\max}+\sigma_{\min})}{2} \tag{8}$$

$$S_m^{'} = S_m \quad (S_a^{'}+S_m \le \sigma_Y) \tag{9a}$$

$$S_m^{'} = \sigma_Y - S_a^{'} \quad (S_a^{'}+S_m > \sigma_Y \quad \text{and} \quad S_a^{'} \le \sigma_Y) \tag{9b}$$

$$S_m^{'} = 0 \quad (S_a^{'} > \sigma_Y) \tag{9c}$$

$$\sigma_a^{'} = \frac{S_a^{'}\cdot S_u}{S_u - S_m^{'}} \tag{10}$$

The relationship between stress concentration factor, K_t, and fatigue notch factor, K_f, can be described in terms of the material notch sensitivity, q as shown in Eq.(11)~(12).

Table 3 Variables and values for calculating the alternating stress intensity revised

a	0.179	Material characteristic length
r_1	0.83	Notch root radius with one-stage process
r_2	0.17	Notch root radius with two-stage process
K_t	1.84	Stress concentration factor
K_{f1}	1.69	Fatigue notch factor with one-stage process
K_{f2}	1.41	Fatigue notch factor with two-stage process

Table 4 Theoretical results according to heading process

	Shape of folding defect	Improved shape of folding
S_m	686.90MPa	281.69MPa
S_a	562.00MPa	230.49MPa
$S_a^{'}$	474.89MPa	162.50MPa
$S_m + S_a^{'}$	1161.79MPa	444.19MPa
$S_m^{'}$	125.11MPa	281.69MPa
$\sigma_a^{'}$	578.23MPa	271.93MPa

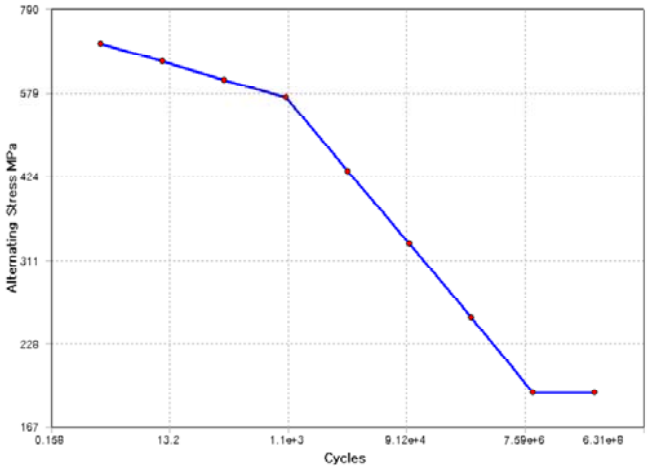

Fig. 17 S-N curve of ST_52

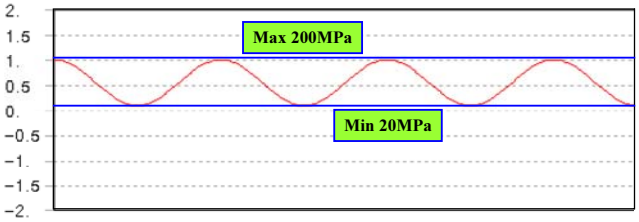

Fig. 18 Amplitude loading ratio of fatigue analysis in FEM

$$K_f = 1+q(K_t-1) \tag{11}$$

$$q=\frac{1}{1+a/r} \quad \text{or} \quad K_f = 1+\frac{K_t-1}{1+a/r} \tag{12}$$

a is the material characteristic length, and r is the notch root radius. Values for a are given by Peterson. The relationship between S_u and a for steel is given as Eq. (13).[16]

$$a = 0.0254\left(\frac{2070}{S_u}\right)^{1.8} \tag{13}$$

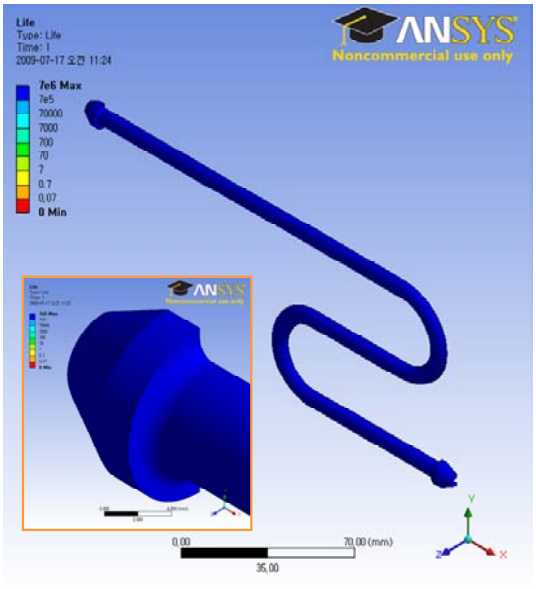

(a) Shape of folding defect (external surface)

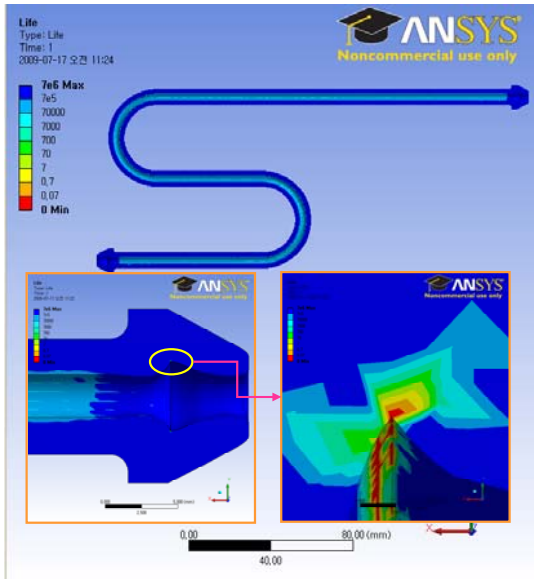

(b) Shape of folding defect (internal surface)

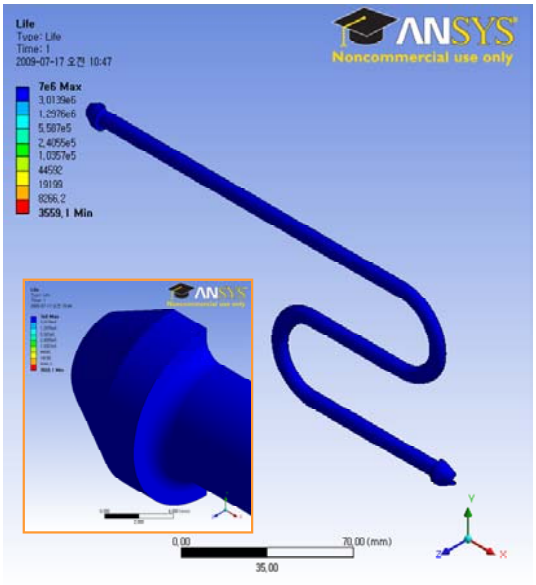

(c) Improved Shape of folding defect (external surface)

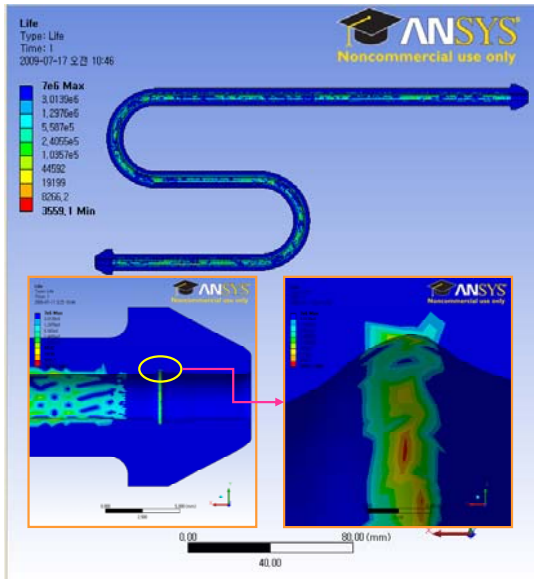

(d) Improved Shape of folding defect (internal surface)

Fig. 19 fatigue life carried out in the fatigue analysis

The variables required for calculating modified alternating stress applied in the pipe before and after improvement of the heading process are shown in Table 3.[17] The results by theoretical analysis are shown in Table 4.

From the S-N curve shown in Fig. 17, fatigue life is calculated by modified alternating stress according to each internal shape.[18] In the current heading process, the minimum fatigue life is 759Cycle and in the improved heading process, it is increased up to 53,850Cycle. So, it seems that fatigue life is improved by changing a one-stage heading process into a two-stage heading process.

5.2 FE-Analysis

5.2.1 Modeling and Boundary condition

The fatigue analysis is performed through the use of structural analysis, and Goodman equation is adopted for calculating of theoretical fatigue life. Fatigue load is obtained from the condition of stability test. Based on the load (200MPa) applied in the structural analysis, the amplitude range of inner pressure is 0.1~1 times, and the repetition interval is 15Hz as shown in Fig. 18.

5.2.2 Analysis Result and Discussion

The results of fatigue analysis are shown in Fig. 19 and Table 5. In the one-stage heading process, fatigue life of the folding part is locally zero in the FEM simulation but is 795cycle in the theory analysis. On the other hand, in the two-stage heading process, the minimum fatigue life increases up to 3,559 sec. So, the two-stage heading process is necessary for stability and improvement of the fatigue life. Also, the results of computer simulations are in good agreement with those of theoretical analysis within 5.6% error. These are just simulation results and some experiments would be required in this study.

Table 5 Comparison the fatigue life from the theoretical analysis and FEM simulation

	FEM simulation	Theory analysis
	Min cycle	Min cycle
Shape of folding defect (one-stage)	Occurrence of crack (0)	759
Improved shape of folding (two-stage)	50,844	53,850

6. Conclusions

In this study, the existing heading process was analyzed, and the current one-stage heading process was modified to a two-stage heading process. In order to satisfy the diameter size of the folding zone with the standard, the optimal design of preform punch and the structural-fatigue coupled field analysis of the fuel oil supply pipe in the common rail system were carried out through the Taguchi method and FEM, and the results of those are summarized as follows.

1. FEM for the final heading process was carried out to obtain smaller folding diameter (3.34mm) than the current folding diameter (4.66mm).
2. The optimal design suggested in this study can be considered to help the prevention of folding defects in the heading process, which uses materials with different diameters and thickness.
3. The structural analysis according to the current and improved heading processes is performed. In the current heading process (a one-stage process), the stress concentration occurs at the end of folding zone where the maximum stress is 1,248MPa, but in the improved heading process (a two-stage process), the maximum stress, 512.19MPa, is reduced by more than 50%.
4. The fatigue analysis according to the current and improved heading process is performed. In a one-stage heading process, the minimum fatigue life is locally zero at the folding part and is pretty high over all area except for the folding part. On the other hand, in a two-stage heading process, the minimum fatigue life increase up to 53,850 cycles.
5. The theoretical analysis result of fatigue life according to a two-stage heading process is 53,850 cycles and in good agreement with those of FEM analysis within 5.6% error.

ACKNOWLEDGEMENTS

This research was financially supported by the Ministry of Education, Science Technology (MEST) and Korea Institute for Advancement of Technology (KIAT) through the Human Resource Training Project for Regional Innovation. And this work is the outcome of a Manpower Development program for Energy & Resources supported by the Ministry of Knowledge and Economy (MKE).

REFERENCES

1. Flaig, U., Polach, W. and Ziegler, G., "Common rail system (CR-system) for passenger car DI diesel engines; Experiences with applications for series production projects," SAE Paper No. 1999-01-0191, 1999.
2. Wang, Z., Lu, J. and Wang, Z. R., "Numerical and experimental research of the cold upsetting-extruding of tube flanges," Journal of Material Processing Technology, Vol. 110, No. 1, pp. 28-35, 2001.
3. Hua, X. L. and Wang, Z. R., "Numerical simulation and experimental study on the multi-step upsetting of a thick and wide flange on the end of a pipe," Journal of Material Processing Technology, Vol. 151, No. 1-3, pp. 321-327, 2004.
4. Lin, S. Y., "Analysis of the Dissimilar Interface Frictional Constraints during the Upsetting Process," International Journal of Advanced Manufacturing Technology, Vol. 13, No. 9, pp. 601-610, 1997.
5. Lee, E. W., "Fatigue Analysis of Pressure Vessles pursuant to ASME Code," Transactions of Korean Society of Steel Construction, Vol. 8, No. 1, pp. 32-38, 1996.
6. Han, S. M., Hwang, B. C., Kim, H. Y. and Kim, C., "Analysis of the Autofrettage Effect in Improving the Fatigue Resistance of Automotive CNG Storage Vessels," Int. J. Precis. Eng. Manuf., Vol. 10, No. 1, pp. 15-21, 2009.
7. ISO/CD 13296, "Diesel engines -- High pressure fuel injection pipe assemblies -- General requirements and dimensions," 2005.
8. Poursina, M., Parvizian, J. and Antonio, C. A. C., "Optimum pre-form dies in two-stage forging," Journal of Material Processing Technology, Vol. 174, No. 1-3, pp. 325-333, 2006.
9. Moe, P. T., Abtahi, S., Ganesan, S. M., Støren, S. and Rudd, W., "Optimization of a pipe end upsetting process," International Journal of Material Forming, Vol. 1, No. 1, pp. 13-16, 2008.
10. Sheu, J. J. and Yu, C. H., "Preform and forging process designs based on geometrical features using 2D and 3D FEM simulations," International Journal of Advanced Manufacturing Technology, Vol. 44, No. 3-4, pp. 244-254, 2008.
11. Gökler, M. I., Darendeliler, H. and Elmaskaya, N., "Analysis of tapered preforms in cold upsetting," International Journal of Machine Tools and Manufacture, Vol. 39, No. 1, pp. 1-16, 1999.
12. Ross, P. J., "Taguchi techniques for quality engineering: loss function, orthogonal experiments, parameter and tolerance design, 2nd Edition," McGraw-Hill, 1996.
13. Li, B., Nye, T. J. and Metzger, D. R., "Multi-objective optimization of forming parameters for tube hydroforming process based on the Taguchi method," International Journal of Advanced Manufacturing Technology, Vol. 28, No. 1-2, pp. 23-30, 2006.

14. Lee, Y. B., "Introduction to Fatigue Analysis," Cheongmoongak, pp. 30-31, 2005.

15. Kim, H. Y., Hwang, B. C., Bae, W. B., Han, S. M. and Kim, C., "Analysis of an Autofrettage Effect to Improve Fatigue Life of the Automotive CNG Storage Vessel," Korean Society for Technology of Plasticity, Vol. 17, No. 4, pp. 292-301, 2008.

16. Stephens, R. I., Fatemi, A., Stephens, R. R. and Fuchs, H. O., "Metal Fatigue in Engineering, 2nd ed.," John Wiley and Sons Inc, pp. 197-198, 2001.

17. Pilkey, W. D., "Peterson's stress concentration factors, 2nd ed.," John Wiley and Sons Inc., p. 436, 1997.

18. Bishop, N. W. M. and Sherratt, F., "Finite element based fatigue calculations," NAFEMS, pp. 31-33, 2000.